Tight Hydrophobic Contacts with the SecB Chaperone Prevent Folding of Substrate Proteins

Bechtluft, Philipp; Kedrov, Alexej; Slotboom, Dirk-Jan; Nouwen, Nico; Tans, Sander J.; Driessen, Arnold J. M.

Published in:
Biochemistry

DOI:
10.1021/bi902051e

Publication date:
2010

2380 *Biochemistry* **2010,** *49,* 2380–2388
DOI: 10.1021/bi902051e

BIOCHEMISTRY
including biophysical chemistry & molecular biology
Article

Tight Hydrophobic Contacts with the SecB Chaperone Prevent Folding of Substrate Proteins[†]

Philipp Bechtluft,[‡] Alexej Kedrov,[‡] Dirk-Jan Slotboom,[§] Nico Nouwen,[∥] Sander J. Tans,[⊥] and Arnold J. M. Driessen*[,‡]

[‡]*Department of Molecular Microbiology, Groningen Biomolecular Sciences and Biotechnology Institute and Zernike Institute for Advanced Materials, University of Groningen, Kerklaan 30, 9751 NN Haren, The Netherlands,* [§]*Department of Membrane Enzymology, Biomolecular Sciences and Biotechnology Institute, University of Groningen, Nijenborgh 4, 9747 AG Groningen, The Netherlands,* [∥]*Laboratoire des Symbioses Tropicales et Méditerranéennes, Campus International de Baillarguet, TA 10/J, 34398 Montpellier cedex 5, France, and* [⊥]*FOM Institute for Atomic and Molecular Physics, Kruislaan 407, 1098 SJ Amsterdam, The Netherlands*

Received December 1, 2009; Revised Manuscript Received February 9, 2010

ABSTRACT: The molecular chaperone SecB binds to hydrophobic sections of unfolded secretory proteins and thereby prevents their premature folding prior to secretion by the translocase of *Escherichia coli*. Here, we have investigated the effect of the single-residue mutation of leucine 42 to arginine (L42R) centrally positioned in the polypeptide binding pocket of SecB on its chaperonin function. The mutant retains its tetrameric structure and SecA targeting function but is defective in its holdase activity. Isothermal titration calorimetry and single-molecule optical tweezer studies suggest that the SecB(L42R) mutant exhibits a reduced polypeptide binding affinity allowing for partial folding of the bound polypeptide chain rendering it translocation-incompetent.

The translocation of proteins across membranes is an essential process in life. In bacteria, a large number of proteins have to cross the cytoplasmic membrane to fulfill their function at the outer surface of the cell or in the extracellular medium. Many of these proteins are synthesized as precursors with an N-terminal signal sequence that is used for correct targeting to the Sec translocase at the membrane. The Sec translocase is a complex of the ATP-driven motor protein SecA and the heterotrimeric SecYEG protein that functions as a membrane-embedded translocation channel (*1*). This pore allows passage of proteins in an unfolded state only. As most proteins rapidly fold after or during synthesis, preproteins have to be maintained in a translocation competent state (i.e., a collective assignment of folding states that are compatible with translocation) in the cytosol prior to their translocation. Alternatively, the process of protein synthesis and translocation can be coupled (cotranslational translocation), thereby preventing premature folding. In *Escherichia coli*, most preproteins are first synthesized to their full length, and once released by the ribosome, they are translocated via the Sec translocase (i.e., post-translational translocation) (*2*). To prevent folding and aggregation, post-translational translocation is assisted by molecular chaperones. In *E. coli* and other proteobacteria (*3*), SecB is an export-dedicated molecular chaperone. First, SecB acts as a holdase by binding to unfolded preproteins, thereby preventing them from stably folding and/or aggregating. Second, SecB associates with SecA, and through this targeting function, SecB contributes to the efficiency of translocation. In addition, SecB is required for the translocation of a subset of type I secretion substrates (*4*).

The crystal structures of SecB of *Haemophilus influenza* (*5*) and *E. coli* (Figure 1) (*6*) provide insights into how SecB might fulfill its dual function in translocation. SecB is a tetrameric chaperone that consists of four identical 17 kDa subunits (*7*, *8*). Each monomeric unit contains a four-strand antiparallel β-sheet followed by a pair of antiparallel α-helices. The dimer is formed by a 180° rotation of one monomer with respect to the other. As a result of this pairing, there is a surface-exposed antiparallel β-sheet on one face of each of the SecB dimers, which provides a high-affinity binding site for the C-terminal tail of SecA. The SecB tetramer is formed by two dimers that form a sandwich with four long α-helices between the eight-strand antiparallel β-sheets at the dimer−dimer interface. The tetramer is very stable with a tetramer−dimer dissociation constant (K_d)[1] of ∼20 nM at pH 7.6 (*9*). Since the cellular SecB concentration is ∼13 μM (*10*), SecB will be a tetramer under physiological conditions. On opposite sides of the SecB tetramer a long peptide binding groove is present. Each peptide binding groove is composed of two peptide binding subsites. Subsite 1 is localized in the deep section of the groove and is formed by mostly aromatic residues that are conserved in the SecB proteins. This subsite likely binds exposed hydrophobic and aromatic regions of the non-native substrate. Subsite 2 is localized in the shallow part of the peptide binding groove and may interact with the main chain of substrate proteins. Conformational variation of the subsites in the different crystal structures points to a structural flexibility of this region

[†]This work was supported by the Organization for Fundamental Research on Matter (FOM) and the Foundation for Life Sciences (ALW), which are both financially supported by The Netherlands Organization for Scientific Research (NWO), The Netherlands Foundation for Scientific Research, Chemical Sciences, and NanoNed, a national nanotechnology program coordinated by the Dutch Ministry of Economic Affairs.

*To whom correspondence should be addressed. E-mail: a.j.m.driessen@rug.nl. Phone: +31-50-3632164. Fax: +31-50-3632154.

[1]Abbreviations: BPTI-CAM, carboxymethylated bovine pancreas trypsin inhibitor; ITC, isothermal titration calorimetry; GdnCl, guanidinium chloride; GST, glutathione *S*-transferase; K_a, association constant; K_d, dissociation constant.

 Published on Web 02/10/2010

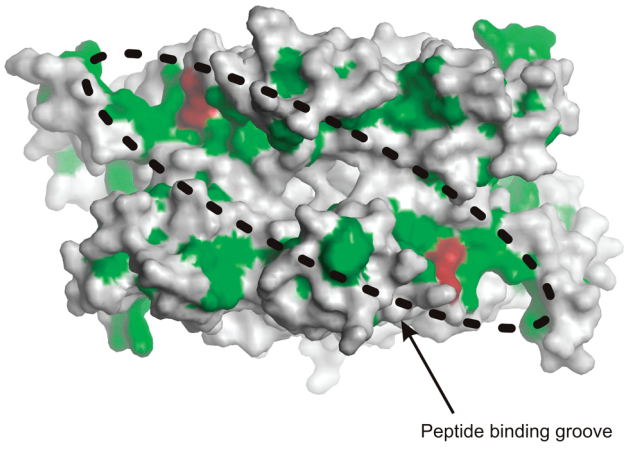

FIGURE 1: Solvent-accessible surface of the SecB tetramer (Protein Data Bank entry 1QYN) with the hydrophobic surface colored green and the position of leucine 42 colored dark red. The proposed peptide binding groove is encircled.

that may serve to provide the required plasticity for binding of peptides with various amino acid compositions.

SecB binds non-native preproteins with a K_d between 5 and 50 nM (*11*, *12*). Protease protection experiments with the substrate proteins maltose binding protein (MBP) and galactose binding protein (GBP) showed that SecB binds to extended protein regions of ~150−170 residues in the mature domain (*13*, *14*). On the basis of these experiments and the known structure of folded MBP and GBP, a ligand binding model for SecB was proposed (*11*) in which there are two types of structures that can be bound by SecB: flexible, extended polypeptide stretches ~15 residues in length and hydrophobic regions corresponding to the core regions of the folded protein structure that are exposed in only the non-native state. Initial binding of the substrate may occur via the short flexible polypeptide stretches and subsite 2 whereupon a conformational change in SecB would expose subsite 1 of the peptide binding groove for tighter ligand binding through interactions with hydrophobic regions in the substrate. An extensive peptide scanning study (*10*) suggested that the SecB polypeptide binding motif is approximately nine amino acid residues long and enriched in aromatic and basic residues, while acidic residues are strongly disfavored. Such SecB binding regions are typically found to be buried in the inner, hydrophobic core of proteins. This explains why SecB binding prevents folding. This model, however, does not explain the specificity of SecB for preproteins as compared to cytosolic proteins since the binding motifs are found theoretically every 20−30 amino acid residues in all protein sequences. Therefore, the selectivity for substrate binding by SecB was suggested to occur by kinetic partitioning of substrates between protein folding and SecB association (*15*).

Previously, mutants of SecB that are defective in preprotein binding have been isolated (*9*, *16*). However, all these mutants have point mutations (Cys76, Val78, and Gln80) in the β-sheets that form the dimer−dimer interface. Consequently, the alterations cause a destabilization of the tetramer, yielding SecB dimers under physiological conditions that inherently affect substrate binding as the long peptide binding grooves are localized at the dimer−dimer interface (*9*). Remarkably, these mutants barely show a defect in protein translocation in vivo, and a reduction in the translocation rates is observed only when a preprotein substrate is analyzed with an additional signal sequence mutation (*16*). Site-directed spin labeling has been used to precisely map the sites of interaction between preproteins and SecB (*17*). The amino acid residues that become constrained upon preprotein binding mostly map in the proposed peptide binding sites of SecB. To analyze the effect of a defective substrate binding to SecB without disrupting the SecB quaternary structure, we introduced a positive charge in the second (hydrophobic) subsite of the peptide binding groove of SecB at a residue that was shown to become constrained upon preprotein binding and that thus likely participates in the binding mechanism. Functional and biochemical characterization of the resulting SecB(L42R) mutant shows that it retains its tetrameric organization and ability to interact with SecA. However, the mutant exhibits a reduced binding affinity for protein substrates and is unable to prevent their folding which means that preproteins rapidly acquire a translocation incompetent state even in the presence of SecB.

MATERIALS AND METHODS

Materials. SecB (*18*), preMBP (*19*), proOmpA (*20*), and 4MBP (*19*) were purified as described previously. Inner membrane vesicles (IMVs) were derived from *E. coli* SF100 cells (*21*).

SecB-GST218 Binding Studies. Purified GST218, a fusion protein of glutathione *S*-transferase and the most distal 22 amino acid residues of SecA (*22*), or GST (8 μg each) was preincubated with SecB or SecB(L42R) (16 μg each) at room temperature for 10 min in 100 μL of PBS buffer [140 mM NaCl, 2.7 mM KCl, 10 mM Na_2HPO_4, and 1.8 mM KH_2PO_4 (pH 7.3)]. Next, the mixture was supplemented with 50 μL of prewashed glutathione-conjugated Sepharose 4B beads, incubated for 15 min at room temperature, and collected by centrifugation. The supernatant with unbound material was removed and precipitated with 5% trichloric acid (TCA). The beads were washed three times with 100 μL of PBS buffer, whereupon bound material was released by incubation with 100 μL of PBS buffer supplemented with 10 mM reduced glutathione. After centrifugation, the eluted supernatant fraction was precipitated with 5% TCA, washed with acetone, and analyzed via 10% SDS−PAGE (*22*).

In Vitro Translocation. Single-cysteine mutants of preMBP and proOmpA were labeled with fluorescein-maleimide as described previously (*23*). Translocation assays were performed in 50 mM HEPES-KOH (pH 7.5), 5 mM $MgCl_2$, 50 mM KCl, 2 mM DTT, 0.1 mg/mL bovine serum albumin (BSA) containing 53 μg/mL wild-type SecB or SecB(L42R) mutant, 140 μg/mL SecA, and 500 μg/mL IMVs. The translocation mixture was supplemented with 10 mM creatine phosphate and 50 μg/mL creatine kinase whereupon urea-denatured preMBP (25 μg/mL) was added. Translocation was started by addition of 1 mM ATP, and the mixture was incubated at 37 °C. Reactions were stopped after 15 min when the mixtures were chilled in an ice−water bath. To remove protease resistant nontranslocated preMBP, 50 μL of the reaction mixture was layered on a 200 μL sucrose cushion [0.2 M sucrose, 50 mM HEPES-KOH (pH 7.5), 50 mM KCl, and 5 mM $MgCl_2$] and centrifuged for 30 min at 70000 rpm in a TLA 120.1 rotor at 4 °C. IMVs were resuspended in 50 μL of 50 mM HEPES-KOH (pH 7.5), 50 mM KCl, and 5 mM $MgCl_2$ and treated with proteinase K (0.1 mg/mL). After 30 min on ice, the protease was inactivated with 1 mM PMSF and the protease-protected material was precipitated with 5% TCA, washed with ice-cold acetone, and analyzed via 12% SDS−PAGE and in-gel fluorescence using a Roche Lumi Imager F1 (Roche Molecular

Biochemicals). In vitro translocation of fluorescein-maleimide-labeled proOmpA was performed as described by de Keyzer et al. (*23*).

Light Scattering Analysis of Protein Aggregation. The aggregation of proOmpA and disaggregation of MBP during refolding were followed by monitoring the changes in the direct light scatter intensity at 320 nm using an Aminco Bowman Series 2 spectrophotometer (SLM Instruments). All solutions were filtered through a 0.22 μm filter. Stock protein and other solutions were centrifuged before use to remove any insoluble matter. To follow the disaggregation of MBP microaggregates, 200 μM unfolded MBP in 3 M GdnCl was diluted 100-fold into refolding buffer [10 mM HEPES-KOH (pH 7.5) and 150 mM NaCl] in the absence and presence of wild-type SecB or the SecB(L42R) mutant, and the light scatter was monitored over time (*24*). For the proOmpA aggregation assay, unfolded proOmpA (40 μM) in 6 M urea was diluted 20-fold in refolding buffer and aggregation monitored as described above.

Size Exclusion Chromatography Combined with Static Light Scattering. Wild-type SecB or SecB(L42R) mutant (200 μL, ~0.5 mg/mL) was applied on a Superdex 200 10/300GL gel filtration column (GE Healthcare) and eluted at a flow rate of 0.5 mL/min in a buffer containing 50 mM Tris-HCl (pH 7.5) and 100 mM KCl using an Agilent 1200 series isocratic pump at room temperature. Detectors were used for the absorbance at 280 nm (Agilent), static light scattering (miniDawn TREOS Wyatt), and differential refractive index (Optilab Rex Wyatt). For data analysis, ASTRA version 5.3.2.10 was used (Wyatt), with a value for the refractive index increment $[(dn/dc)_{protein}]$ of 0.187 mL/mg (*25*, *26*).

Fluorescence and Circular Dichroism Spectroscopy. SecB variants were prepared in 100 mM potassium phosphate buffer (pH 7.5) at concentrations of ~50 μM for intrinsic fluorescence measurements and 10 μM for circular dichroism. Precise sample concentrations were determined on the basis of their light absorbance using an extinction coefficient at 280 nm of 13200 M^{-1} cm^{-1}. The intrinsic fluorescence of SecB variants was recorded at 25 °C using an SLM Aminco spectrofluorometer, with an excitation wavelength of 280 nm (slit width of 2 nm). Fluorescence spectra were recorded from 300 to 450 nm (slit width of 2 nm) at a rate of 1 nm/s. Far-UV CD spectra of the SecB variants were recorded at 25 °C on an Aviv 62A DS spectrophotometer over the wavelength range from 195 to 250 nm with a rate of 1 nm/s. Reference spectra were recorded for both intrinsic fluorescence and CD with the buffer solution in the absence of the protein and subtracted from the SecB spectra.

Isothermal Titration Calorimetry. Slow-folding mutant preMBP(A276G) was used to study interactions of the SecB variants with natural substrates. Immediately prior the ITC experiment, the protein was transferred into buffer solution containing 150 mM potassium acetate, 10 mM HEPES, and 0.5 M GdnCl (pH 7.6) using a PD-10 desalting column (GE Healthcare). BPTI was used as a model substrate to study SecB binding at the elevated temperature. To achieve the stable unfolded conformation of BPTI, denatured and reduced protein was treated with iodoacetamide as described to achieve the BPTI-CAM form (*18*). The denaturing solution was then exchanged for 100 mM potassium phosphate buffer (pH 7.4) via a PD-10 column. SecB was transferred into the corresponding solution using Micro BioSpin 6 columns (Bio-Rad). Samples were centrifuged prior to the ITC experiment, and concentrations were determined on the basis of their light absorbance using the following extinction coefficients at 280 nm: 13200 M^{-1} cm^{-1} for SecB variants, 60500 M^{-1} cm^{-1} for preMBP, and 6300 M^{-1} cm^{-1} for BPTI.

ITC experiments were conducted using an ultrasensitive ITC_{200} calorimeter (MicroCal). SecB variants (approximately 40 μL) at concentrations of 200−400 μM (calculated for the monomer) were titrated into the thermally equilibrated ITC cell filled with ~200 μL of the substrate solution at concentrations of 5−20 μM. Titrations were performed at 6 °C for preMBP and 25 °C for BPTI and were repeated at least three times. Control measurements included titration of each SecB variant into the buffer solution, and the buffer into the cell with the substrate. Data were analyzed using the ORIGIN-based software provided by MicroCal.

Optical Tweezer Experiments. A quadruple MBP (4MBP) was mechanically unfolded with optical tweezers by coupling between two polystyrene beads as reported previously (*19*). Wild-type SecB or SecB(L42R) was present during the single-molecule experiments at a final concentration of 0.1 μM. 4MBP was unfolded at a force loading rate of 7 pN/s. Between sequential pulls, a dwell time was introduced in which the tether was maintained for 10 s at zero loading force. The sequential force extension unfolding curves of four individual 4MBP molecules (11 in the presence of the wild-type and 15 in the presence of L42R) were evaluated on structural features or showing no tertiary structure at all. The statistical significance of the data from a Student's *t* test for small unequal sample sizes with equal variance yielded a *t* value of 2.5020, which relates to a confidence index of $>95\%$.

Other Methods. Protein concentrations were determined using a DC protein assay kit (Bio-Rad) with BSA as a standard.

RESULTS

Structure of the SecB(L42R) Mutant. To analyze the effect of a defective substrate binding site without alteration of the quaternary structure of SecB, we introduced a positive charge (L42R) in the center of subsite 2 of the peptide binding groove of SecB (Figure 1). We choose the second substrate binding subsite as it contains mainly hydrophobic residues, and introducing a positive charge in the center is expected to drastically affect peptide binding because it has been shown that the leucine residue at position 42 becomes highly constrained when SecB associates with a peptide substrate (*17*). The SecB(L42R) mutant was overexpressed in *E. coli* and purified to homogeneity. Circular dichroism (Figure 2A) and tryptophan fluorescence spectroscopy (Figure 2B) demonstrate that the mutation does not affect the secondary and tertiary structure of SecB. Size exclusion chromatography in combination with static light scattering analysis (*25*) showed that wild-type SecB and SecB(L42R) elute as a single homogeneous peak from the size exclusion column and have calculated molecular masses of 71.5 and 71.7 kDa, respectively (Figure 2). As the theoretical molecular mass of tetrameric SecB is 69.1 kDa, it is concluded that SecB(L42R) retains the native quaternary organization.

SecB(L42R) Binds to the Carboxyl Terminus of SecA. SecB targets preproteins to SecA by binding with high affinity to the extreme carboxyl terminus of SecA. To investigate if the mutant SecB interacts with SecA, we analyzed the binding of SecB(L42R) to glutathione *S*-transferase to which the last 21 carboxyl-terminal residues of *E. coli* SecA are fused (GST218) (*22*). When bound to glutathione beads, GST218 specifically pulls down SecB(L42R) (Figure 3, lane 9) and does

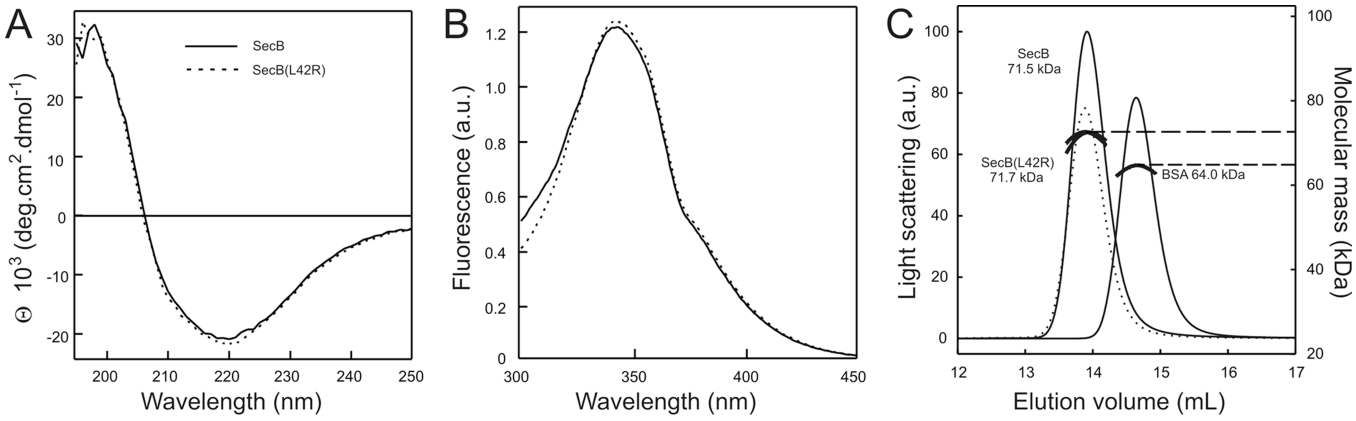

FIGURE 2: Circular dichroism (A), intrinsic fluorescence spectroscopy (B), and size exclusion chromatography and light scatter detection (C) of wild-type SecB (—) and SecB(L42R) (---) confirm a conservation of SecB secondary, tertiary, and quaternary structure upon introduction of a charged residue in the hydrophobic moiety in the SecB(L42R) mutant. Bovine serum albumin was used as an internal standard during size exclusion chromatography.

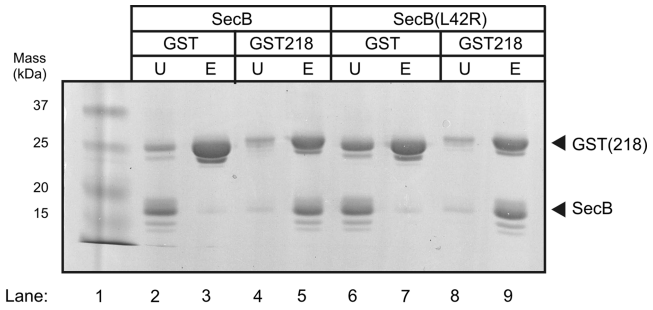

FIGURE 3: Binding of wild-type SecB (lanes 2−5) and the SecB(L42R) mutant (lanes 6−9) to the extreme carboxyl terminus of SecA. GST and GST218 were incubated with the SecB variants, and complexes were isolated with glutathione-coupled agarose beads. Unbound material was removed (U, lanes 2, 4, 6, and 8); beads were washed, and GST (E, lanes 3 and 7) and GST218 (E, lanes 5 and 9) were eluted from the beads with reduced glutathione.

not interact with control glutathione *S*-transferase (Figure 3, lane 6). Wild-type SecB also interacts with GST218 (Figure 3, lanes 2−5), consistent with previous results (*22*, *27*). These data demonstrate that the interaction of SecB(L42R) with the high-affinity binding site of SecA is not disturbed.

SecB(L42R) Is Hindered in Maintaining Preproteins in a Translocation Competent State. To analyze the impact of the L42R mutation on preprotein translocation, in vitro translocation assays were performed using the model precursors of the maltose binding protein (preMBP) and outer membrane protein A (proOmpA) as substrates. Unlike proOmpA translocation that is stimulated by SecB, preMBP translocation is strictly dependent on SecB. Urea-denatured fluorescently labeled preMBP or proOmpA was diluted into translocation buffer containing SecB, where after the translocation the reaction was started by the addition of SecA, ATP, and *E. coli* inner membrane vesicles (IMVs). The amount of translocated preMBP and proOmpA within 15 min of incubation was visualized by SDS−PAGE and in-gel fluorescence after removal of the nontranslocated preprotein by proteinase K digestion. When the translocation reaction was started directly after dilution of preMBP into translocation buffer containing SecB, only a slight reduction in translocation efficiency was observed with the SecB(L42R) mutant as compared to wild-type SecB (Figure 4A, lane 3 vs lane 2). In the absence of SecB, only low levels of preMBP were translocated (Figure 4A, lane 4). This demonstrates that Sec(L42R) still supports the SecB-dependent translocation of preMBP, consistent with the notion that this mutant can target preproteins to SecA.

In another experiment, the preMBP diluted from the denaturant was first incubated for different time intervals in translocation buffer with and without SecB, and subsequently, the translocation competence of the preMBP was tested by the addition of IMVs, SecA, and ATP. These experiments showed a large difference between wild-type SecB and SecB(L42R). Whereas a 30 min preincubation in the presence of wild-type SecB hardly affected the ability of preMBP to translocate (Figure 4B, lanes 2−5), a 15 min preincubation period in the presence of SecB(L42R) resulted in a drastic decrease in the preMBP translocation efficiency (Figure 4B, lanes 7−10). Similar results were obtained with proOmpA. Whereas proOmpA translocation is not strictly dependent on SecB (*28*) (Figure 4C, lane 2 vs lane 6), preincubation of urea-denatured proOmpA in translocation buffer without SecB for 30 min resulted in an almost complete loss of translocation (Figure 4C, lanes 2−4). In contrast, when wild-type SecB was present in the preincubation period, proOmpA remained translocation competent for up to at least 60 min (Figure 4, lanes 6−8). On the other hand, with SecB(L42R), after preincubation periods of 30 min there was already a drastic reduction in the level of proOmpA translocation (Figure 4, lanes 10−12). Collectively, these data show that the SecB(L42R) mutant normally supports the translocation of preproteins that are strictly dependent on SecB but that it is unable to maintain protein substrates in a translocation competent state over longer periods of time.

SecB(L42R) Is Defective in MBP Disaggregation and Unable To Prevent proOmpA Aggregation. The inability to maintain preproteins in a translocation competent state suggests that the chaperone function of SecB is altered due to the L42R mutation. To analyze this in more detail, we analyzed the effect of SecB(L42R) on the folding of the mature region of preMBP, i.e., MBP, and on proOmpA by monitoring the light scattering of these substrates upon dilution from guanidinium chloride (GdnCl). When GdnCl-denatured MBP (final concentration of 200 μM) is diluted into a buffer without SecB, MBP microaggregates that slowly disaggregate in ~10 min are formed, allowing for MBP folding [Figure 5A (◇)]. In the presence of SecB, the disaggregation rate is dramatically enhanced by a factor of up to 10 [Figure 5A (□)]. SecB(L42R) also stimulates

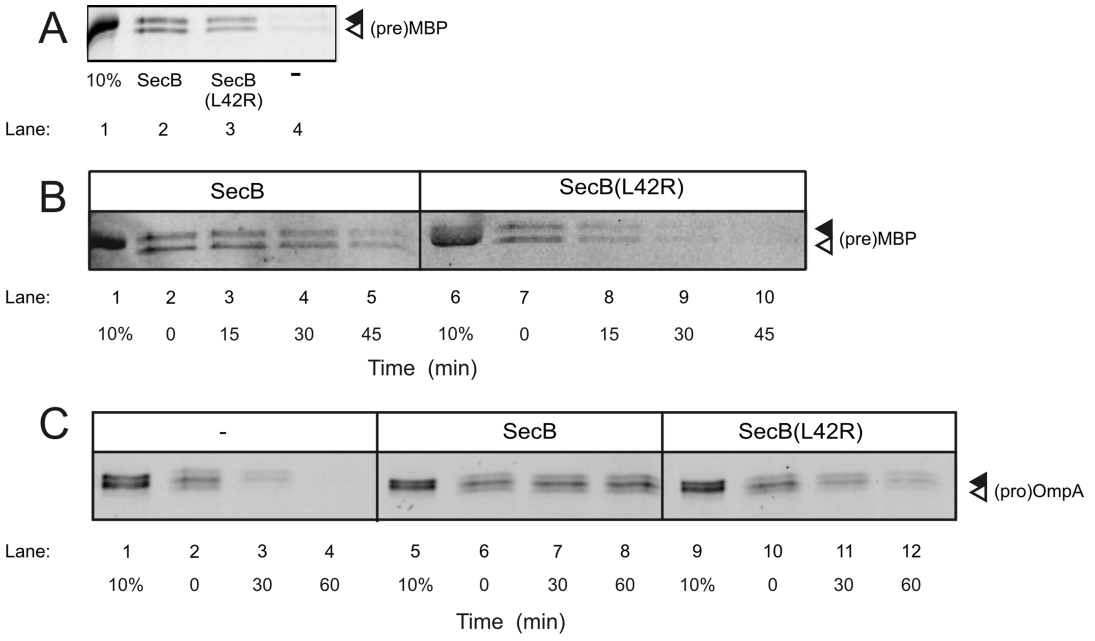

FIGURE 4: In vitro translocation of preMBP and proOmpA. (A) Translocation of preMBP was assayed in the presence of SecB (lane 2) or SecB(L42R) (lane 3) or without SecB (lane 4). The ability of wild-type SecB and SecB(L42R) to maintain preMBP (B) and proOmpA (C) in a translocation competent state was evaluated by incubating the proteins in the translocation assay mixture for the indicated amount of time, whereupon translocation was started with the addition of 1 mM ATP.

disaggregation [Figure 5A (△)], albeit much less efficiently than wild-type SecB. Like MBP, proOmpA diluted from 3 M GdnCl (final concentration of 2 μM) rapidly formed light scattering aggregates, but in contrast to MBP, these aggregates are very stable and do not disaggregate (Figure 5B) (*28*). In the presence of stoichiometric amounts of wild-type SecB, the aggregation of proOmpA was almost completely suppressed [Figure 5B,C (□)], whereas a similar concentration of the SecB(L42R) mutant hardly prevents aggregation [Figure 5B,C (△)]. These results show that the L42R mutation drastically affects the chaperone function of SecB.

The SecB(L42R) Mutant Binds Substrates with a Reduced Affinity. The inability to prevent aggregation and to stimulate disaggregation suggests that the SecB−substrate interaction is altered due to the L42R mutation. To quantitatively measure binding of the substrate to SecB, we measured the thermodynamics of this process using isothermal titration calorimetry (ITC). To this end, a concentrated SecB solution was titrated into a ITC cell containing a slow-folding preMBP-(A276G) mutant at 6 °C, and the effects of heat on the binding reaction were recorded (Figure 6A,B). Like the wild-type, this slow-folding mutant of preMBP is still dependent on SecB for translocation (*29*). Wild-type preMBP was not used in these experiments as it aggregates more rapidly, making measurements unreliable. On the basis of the measured parameters, binding energies and affinity constants for the interaction between SecB variants and preMBP(A276G) were calculated. Both SecB variants bind preMBP(A276G) with a stoichiometry close to 4, indicating that for the natural substrate each tetrameric SecB binds one substrate molecule. However, the association constant, K_a, for the interaction of SecB(L42R) with preMBP is ~2 times lower than that of the wild-type protein, indicating a reduced binding affinity. For both SecB variants, the substrate binding was enthalpy-driven, although in agreement with previous studies a significant enthalpy−entropy compensation was observed (*30*). This nonfavorable decrease in entropy is likely caused by the loss of translational mobility and the reduced rotational mobility of the substrate upon binding to SecB. Despite the overall similarities with wild-type SecB, the L42R mutation decreased the enthalpy contribution (ΔH) to binding energy but also increased the entropic term ($T\Delta S$), suggesting higher flexibility of the chaperone−substrate complex.

To validate that the change in the binding properties of SecB is directly caused by the mutation, but not denaturant or the low temperature, we also studied the interactions of the SecB variants with the unfolded form of bovine pancreatic trypsin inhibitor (BPTI-CAM) at 25 °C (Figure 6C,D). Because of its small size, BPTI-CAM binding is limited to a single monomer within the SecB tetramer, so the stoichiometry observed in ITC experiments was close to 1. SecB(L42R) demonstrated a 4 times lower affinity for the substrate, corresponding to a free energy difference of ~1 kcal/mol. As for preMBP interactions, both the entropy loss and the enthalpy of BPTI-CAM binding were reduced by the mutation within the SecB active site.

The SecB(L42R) Mutant Allows Partial Folding of Proteins. Previously, using optical tweezers, we have shown that SecB prevents folding of MBP to its final stable tertiary structure (*19*). To analyze the direct impact of the SecB mutation on MBP folding, we repeated the single-molecule unfolding experiments with SecB(L42R). To this end, a folded quadruple MBP (4MBP) construct was tethered between two polystyrene beads, one of which is immobilized on a pipet and the other of which is trapped in the optical trap (Figure 7A). When MBP is mechanically unfolded in the presence of the SecB(L42R) mutant by moving one of the polystyrene beads, the first stretching trace of 4MBP shows the common features of a low-force, smooth detachment of the C-terminal α-helices, followed by a sawtooth unfolding of the four MBP core domains (Figure 7B, gray trace). This behavior is similar to the observations for wild-type SecB (Figure 7C). When following a relaxation and a dwell time of 10 s, a second stretching curve in the absence of chaperone resulted in the formation of an aggregate that could only be disrupted at

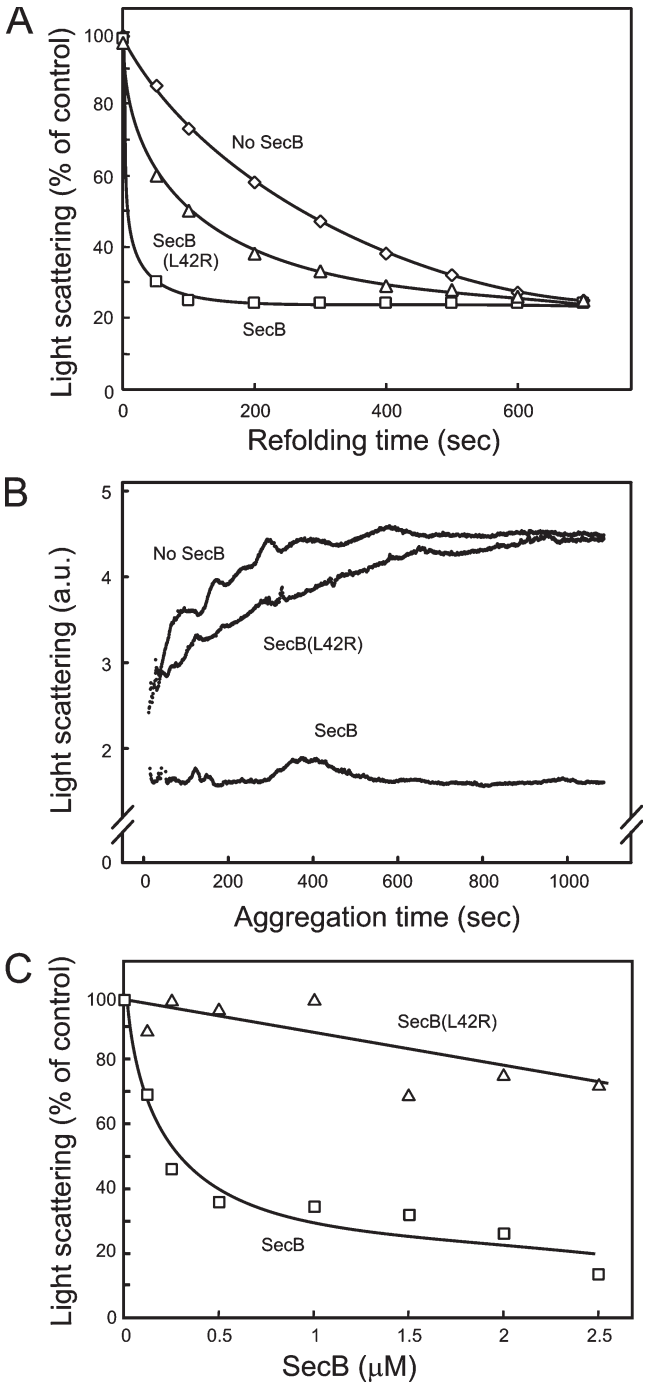

FIGURE 5: (A) Effect of wild-type SecB (□) and SecB(L42R) (△) on the aggregation of MBP during refolding from the GdnCl-denatured state (◇). The final concentrations of MBP and SecB were 2 and 1 μM, respectively. (B) Effect of wild-type SecB and the SecB(L42R) mutant (final concentration of 1 μM) on the kinetics of proOmpA (2 μM) aggregation. (C) Effect of wild-type SecB (□) and the SecB(L42R) mutant (△) on proOmpA aggregation. The relative light scattering levels of urea-diluted proOmpA (2 μM) were measured after incubation for 15 min. Concentrations of SecB are for the homotetramer.

high forces (> 30 pN) (data not shown) (*19*). In the presence of the SecB(L42R) mutant, the second stretching curve did not exhibit these aggregation features. Instead, they typically exhibited unfolding features that involved a discrete number of repeats and unfolding forces in the same range as that of the first unfolding of the native structure (Figure 7B). Whether these features, which were observed in 14 of 15 second stretching curves, originate from partial native structures combined with alternative folds, or only alternative folds, cannot be determined in these experiments. However, these data are in clear contrast with the second stretching curves of 4MBP in the presence of wild-type SecB, which do not show these unfolding features (Figure 7C, black dotted line) (*19*).

DISCUSSION

All of the SecB mutations known to interfere with preprotein binding have been isolated via genetic screens and were shown to always lead to a dissociation of the tetrameric SecB structure into dimers (*9*, *16*). The polypeptide binding sites are organized as long and deep grooves at the dimer−dimer interface, and therefore, the preprotein binding is disrupted in these mutants. Because of a loss of quaternary structure, it is impossible to determine what causes the defect in protein translocation in the selected mutants, i.e., a deficiency in SecA targeting, a defect in the holdase function, or a combination of both. It should, however, be stressed that the in vivo defects in protein translocation with the previously described protein binding mutants is remarkably mild as compared to that with the mutants defective in SecA binding (*16*). Also, to detect the secretion defect, we used a preMBP variant with a signal sequence mutation. Therefore, regular genetic screens likely do not detect mutants with a defect in the holdase function only. To disrupt preprotein binding but to leave the quaternary and thus overall structure of the peptide binding groove of SecB intact, we engineered a nonconserved amino acid substitution (L42R) in the second peptide binding subsite that alters the hydrophobicity and overall charge of the polypeptide binding groove (Figure 1). Since there are four of these subsites on a single SecB tetramer, each of the long polypeptide binding grooves contains two mutations. Our data show that the SecB(L42R) mutant maintains the quaternary structure of SecB (Figure 2C), thus allowing us to study the functional impact of the mutation on the chaperone activity of SecB in protein translocation, aggregation, and folding. Importantly, the mutant exhibits a nativelike interaction with SecA as demonstrated by its ability to specifically bind the proximal 21 carboxyl-terminal residues of SecA fused to glutathione *S*-transferase (Figure 3). Previously, this interaction was shown to be of high affinity and to genuinely mimic SecB−SecA binding at the translocase (*22*). Thus, potential translocation defects of the SecB(L42R) mutant cannot be assigned to a loss of targeting to SecA.

The Sec(L42R) mutant almost normally supports the translocation of preMBP into IMVs of *E. coli*, a process that is strictly dependent on SecB (Figure 4A). However, when GdnCl-unfolded preMBP was incubated in the presence of SecB for a longer period of time prior to translocation, the SecB(L42R) mutant exhibited a strongly reduced ability to maintain preMBP in a translocation competent state (Figure 4B). This suggests that the strict SecB requirement of preMBP translocation can be largely attributed to a function of SecB in the targeting of preMBP to the SecA subunit of the translocase rather than prevention of protein folding or aggregation which occurs at a longer time scale. Indeed, prolonged incubation times in the absence of SecB or the presence of the SecB(L42R) mutants inevitably resulted in a loss of the translocation competence of preMBP. Similar observations were made with the precursor proOmpA that is less dependent on SecB for its translocation but that in the absence of the chaperone readily aggregates (Figure 4C). From these data, we conclude that the

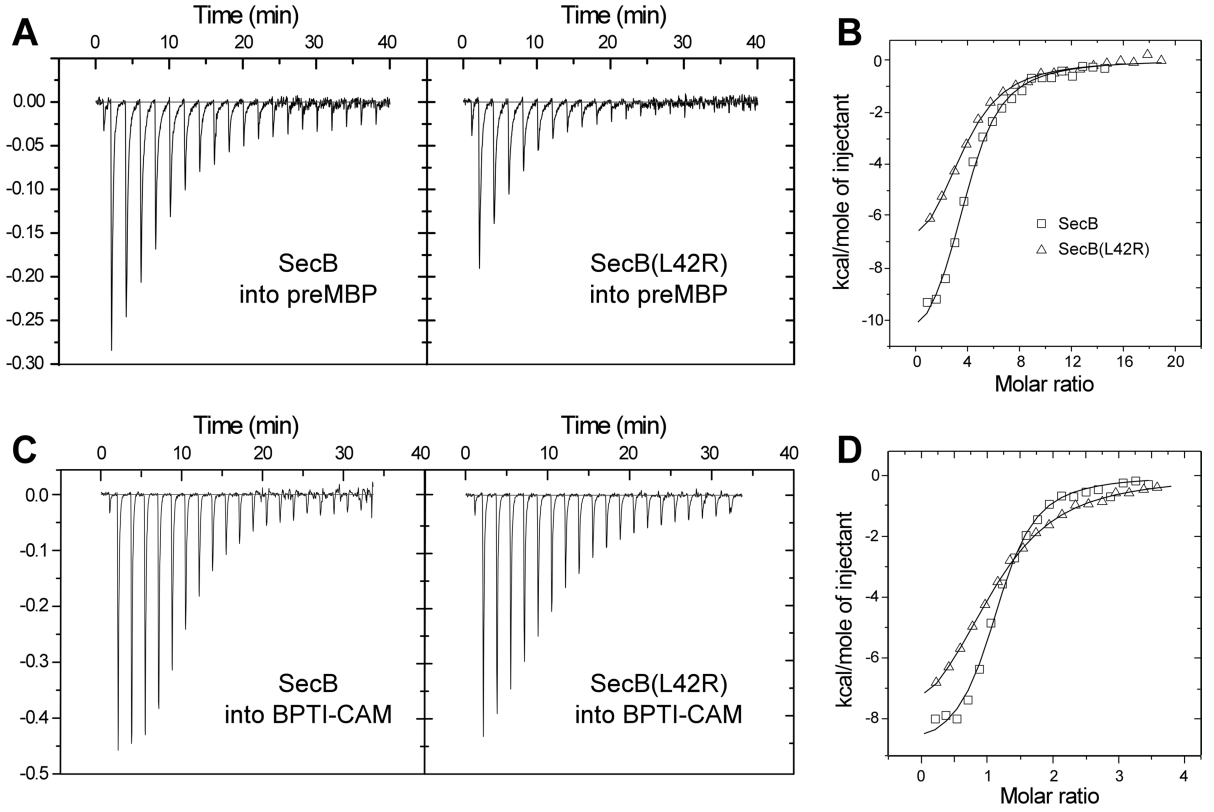

FIGURE 6: SecB−preMBP interactions studied by isothermal titration calorimetry. (A) Binding isotherms of the titration of wild-type SecB and SecB(L42R) (up to 300 μM monomer) with a solution containing 5 μM preMPB(A276G) at 6 °C. For the titrations of wild-type SecB (□) and SecB(L42R) (△) into the preMBP solution, the area under each injection signal was integrated and plotted (B). Interactions of SecB variants with unfolded BPTI-CAM at 25 °C also confirm the change in binding properties upon mutation (C and D). The solid lines in panels B and D represent nonlinear least-squares fits of the reaction heat for the injection. The enthalpy per mole of SecB injected is plotted vs the SecB monomer:substrate ratio.

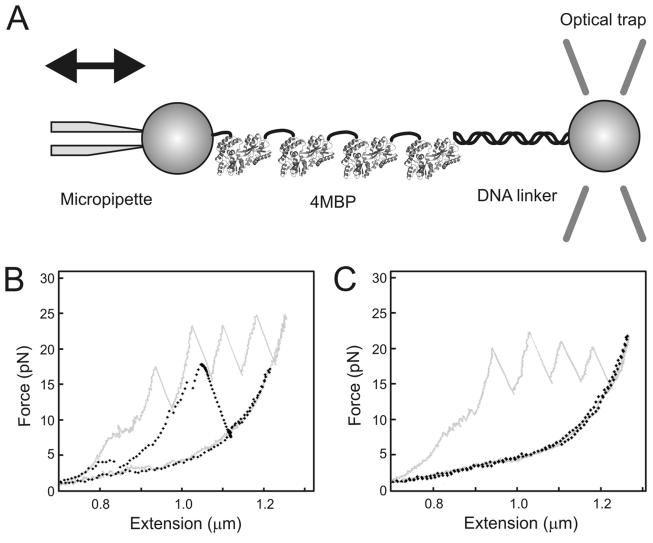

FIGURE 7: Force−extension curves of the mechanical unfolding of a quadruple MBP protein (4MBP). (A) Scheme of the optical tweezers setup with 4MBP at its C-terminus connected via a double-stranded DNA spacer to a polystyrene bead that is trapped by a laser, and with its N-terminus connected to another polystyrene bead fixed on a pipet that can be moved in the *xyz* direction. (B) Force−extension curves in the presence of SecB(L42R) (0.1 μM). First pull (gray solid line) followed by a second pull (black dotted line) after 10 s at zero force load. (C) Force−extension curves in the presence of wild-type SecB (0.1 μM). First extension (gray solid line) and second extension (black dotted line) after 10 s at zero force load.

SecB(L42R)−preprotein complex exhibits a reduced stability as compared to that of wild-type SecB. This conclusion is supported by light scattering experiments that monitor the SecB-dependent disaggregation of preMBP microaggregates and the ability of SecB to prevent the aggregation of proOmpA (Figure 5). Finally, a change in the polypeptide binding properties by the SecB mutant was directly demonstrated by ITC using the stably unfolded form of the small model substrate protein BPTI and a slow-folding variant of the natural substrate preMBP (Figure 6 and Table 1). SecB(L42R) reproducibly demonstrated an up to 4-fold lower binding affinity under different experimental conditions, and the mutation affected both the enthalpic and entropic terms. Interestingly, replacing a hydrophobic residue with a polar residue in the SecB(L42R) mutant reduces the total entropy loss upon substrate binding. A detailed explanation of this phenomenon is difficult in the absence of the structure of the SecB−substrate complex and knowledge of the solvent behavior. However, a possible scenario we suggest is that the substrate retains a certain degree of mobility when bound to the surface of the SecB(L42R) mutant. This will result in a higher entropy of the complex that will partially compensate for the negative change in enthalpy, such that the overall binding affinity change per binding site is relatively small compared to that of wild-type SecB. Overall, the reduced preprotein binding affinity only marginally affects the ability of SecB to support protein translocation. Possibly, the mutation has a more severe effect on the ability of SecB to rescue the growth defect of the trigger factor and DnaK-deficient *E. coli* strain (*31*), or the ability to support translocation of type I secretion system substrates (*4*).

To understand the effect of the reduced binding affinity and thermodynamic considerations described above on the effect of the SecB(L42R) mutant on folding of protein substrates,

Table 1: Thermodynamic Parameters of the Binding of Unfolded preMBP-(A276G) and BPTI-CAM to Wild-Type (WT) SecB and the SecB(L42R) Mutant

		preMBP at 6 °C	BPTI at 25 °C
N^a	WT	4.3	0.9
	L42R	4.4	0.8
K_a ($\times 10^6$ M^{-1})	WT	1.9	0.7
	L42R	1.05	0.15
ΔH (kcal/mol)	WT	−41	−10.5
	L42R	−30	−9.0
$T\Delta S$ (kcal/mol)	WT	−33	−2.6
	L42R	−23	−1.9

[a]Molar ratio of SecB monomer to substrate.

single-molecule experiments were performed using an optical tweezers setup able to monitor the folding and refolding of MBP in the absence and presence of the SecB(L42R) mutant. In this setup, a quadruple fusion protein of MBP (4MBP) was used as this allowed us to monitor two phenomena at the single-molecule level, i.e., protein aggregation and folding (*19*). We have previously shown that when 4MBP is mechanically unfolded in the absence of a chaperone and subsequently in the dwell time following the tweezer relaxation, protein aggregates are formed which is evident from a sharp increase in the unfolding force during the second unfolding reaction. The force required to extend the aggregate exceeds the unfolding force of natively folded MBP. However, in the presence of both wild-type SecB and the SecB(L42R) mutant, this type of aggregation of 4MBP is prevented. This result is consistent with the bulk disaggregation experiments with unfolded MBP. In contrast, the SecB mutant was barely capable of preventing the aggregation of unfolded proOmpA. However, unlike preMBP, proOmpA is unable to spontaneously fold into its native state and readily aggregates, presumably because of its high content of β-strand secondary structure. In the presence of wild-type SecB, 4MBP after relaxation from the extended state typically shows a molten globule-like state (Figure 7C). With SecB(L42R), 4MBP forms neither tight aggregates nor a molten globule-like state. Instead, folds are formed that involve one or more of the MBP repeats, and these structures exhibit an unfolding stability up to that of the native MBP structure. Previous kinetic studies have shown that the SecB polypeptide association rate is diffusion-limited. Since the SecB(L42R) mutant exhibits a reduced protein binding affinity, and hence a less stable SecB−preprotein complex, we assume that the functional defect is due to a faster polypeptide dissociation rate. Consequently, this will allow for a greater time window for the substrate to undergo some refolding before rebinding, explaining the folding signatures in the subsequent unfolding reaction in the optical tweezer experiments. In this respect, substrate folding to the native state when bound to SecB was recently proposed by Krishnan and co-workers (*32*). Tight binding to wild-type SecB largely confines the conformational space available for the bound substrate, thus causing the decline in entropy seen in calorimetric measurements. The SecB(L42R) mutant may permit an enhanced substrate flexibility, which may cause the partial refolding of the bound polypeptide chain. It is, however, unlikely that in the optical tweezer experiments the folded MBP core structures are still bound by SecB. Only after mechanical unfolding, SecB will rebind the unfolded protein.

In summary, these single-molecule studies show a direct impact of the mutation of SecB on the chaperone function and explain the weakened ability of the SecB(L42R) mutant to maintain preproteins in a translocation competent state. Our results also provide support for the proposed SecB−preprotein binding model that implicates hydrophobic interaction at the peptide binding groove as a major force for binding.

ACKNOWLEDGMENT

We thank A. Mashaghi for helpful discussions.

REFERENCES

1. Driessen, A. J., and Nouwen, N. (2008) Protein translocation across the bacterial cytoplasmic membrane. *Annu. Rev. Biochem. 77*, 643–667.
2. Randall, L. L., and Hardy, S. J. (1986) Correlation of competence for export with lack of tertiary structure of the mature species: A study in vivo of maltose-binding protein in *E. coli*. *Cell 46*, 921–928.
3. van der Sluis, E. O., and Driessen, A. J. (2006) Stepwise evolution of the Sec machinery in Proteobacteria. *Trends Microbiol. 14*, 105–108.
4. Delepelaire, P., and Wandersman, C. (1998) The SecB chaperone is involved in the secretion of the *Serratia marcescens* HasA protein through an ABC transporter. *EMBO J. 17*, 936–944.
5. Xu, Z., Knafels, J. D., and Yoshino, K. (2000) Crystal structure of the bacterial protein export chaperone secB. *Nat. Struct. Biol. 7*, 1172–1177.
6. Dekker, C., de Kruijff, B., and Gros, P. (2003) Crystal structure of SecB from *Escherichia coli*. *J. Struct. Biol. 144*, 313–319.
7. Smith, V. F., Schwartz, B. L., Randall, L. L., and Smith, R. D. (1996) Electrospray mass spectrometric investigation of the chaperone SecB. *Protein Sci. 5*, 488–494.
8. Topping, T. B., Woodbury, R. L., Diamond, D. L., Hardy, S. J., and Randall, L. L. (2001) Direct demonstration that homotetrameric chaperone SecB undergoes a dynamic dimer-tetramer equilibrium. *J. Biol. Chem. 276*, 7437–7441.
9. Muren, E. M., Suciu, D., Topping, T. B., Kumamoto, C. A., and Randall, L. L. (1999) Mutational alterations in the homotetrameric chaperone SecB that implicate the structure as dimer of dimers. *J. Biol. Chem. 274*, 19397–19402.
10. Knoblauch, N. T., Rudiger, S., Schonfeld, H. J., Driessen, A. J., Schneider-Mergener, J., and Bukau, B. (1999) Substrate specificity of the SecB chaperone. *J. Biol. Chem. 274*, 34219–34225.
11. Randall, L. L., and Hardy, S. J. (1995) High selectivity with low specificity: How SecB has solved the paradox of chaperone binding. *Trends Biochem. Sci. 20*, 65–69.
12. Topping, T. B., and Randall, L. L. (1997) Chaperone SecB from *Escherichia coli* mediates kinetic partitioning via a dynamic equilibrium with its ligands. *J. Biol. Chem. 272*, 19314–19318.
13. Topping, T. B., and Randall, L. L. (1994) Determination of the binding frame within a physiological ligand for the chaperone SecB. *Protein Sci. 3*, 730–736.
14. Khisty, V. J., Munske, G. R., and Randall, L. L. (1995) Mapping of the binding frame for the chaperone SecB within a natural ligand, galactose-binding protein. *J. Biol. Chem. 270*, 25920–25927.
15. Hardy, S. J., and Randall, L. L. (1991) A kinetic partitioning model of selective binding of nonnative proteins by the bacterial chaperone SecB. *Science 251*, 439–443.
16. Kimsey, H. H., Dagarag, M. D., and Kumamoto, C. A. (1995) Diverse effects of mutation on the activity of the *Escherichia coli* export chaperone SecB. *J. Biol. Chem. 270*, 22831–22835.
17. Crane, J. M., Suo, Y., Lilly, A. A., Mao, C., Hubbell, W. L., and Randall, L. L. (2006) Sites of interaction of a precursor polypeptide on the export chaperone SecB mapped by site-directed spin labeling. *J. Mol. Biol. 363*, 63–74.
18. Fekkes, P., de Wit, J. G., van der Wolk, J. P., Kimsey, H. H., Kumamoto, C. A., and Driessen, A. J. (1998) Preprotein transfer to the *Escherichia coli* translocase requires the co-operative binding of SecB and the signal sequence to SecA. *Mol. Microbiol. 29*, 1179–1190.
19. Bechtluft, P., van Leeuwen, R. G., Tyreman, M., Tomkiewicz, D., Nouwen, N., Tepper, H. L., Driessen, A. J., and Tans, S. J. (2007) Direct observation of chaperone-induced changes in a protein folding pathway. *Science 318*, 1458–1461.
20. Crooke, E., Guthrie, B., Lecker, S., Lill, R., and Wickner, W. (1988) ProOmpA is stabilized for membrane translocation by either purified *E. coli* trigger factor or canine signal recognition particle. *Cell 54*, 1003–1011.
21. Cunningham, K., and Wickner, W. T. (1989) Detergent disruption of bacterial inner membranes and recovery of protein translocation activity. *Proc. Natl. Acad. Sci. U.S.A. 86*, 8673–8677.

22. Fekkes, P., van der Does, C., and Driessen, A. J. (1997) The molecular chaperone SecB is released from the carboxy-terminus of SecA during initiation of precursor protein translocation. *EMBO J. 16*, 6105–6113.
23. de Keyzer, J., van der Does, C., and Driessen, A. J. (2002) Kinetic analysis of the translocation of fluorescent precursor proteins into *Escherichia coli* membrane vesicles. *J. Biol. Chem. 277*, 46059–46065.
24. Ganesh, C., Zaidi, F. N., Udgaonkar, J. B., and Varadarajan, R. (2001) Reversible formation of on-pathway macroscopic aggregates during the folding of maltose binding protein. *Protein Sci. 10*, 1635–1644.
25. Slotboom, D. J., Duurkens, R. H., Olieman, K., and Erkens, G. B. (2008) Static light scattering to characterize membrane proteins in detergent solution. *Methods 46*, 73–82.
26. Folta-Stogniew, E. (2006) Oligomeric states of proteins determined by size-exclusion chromatography coupled with light scattering, absorbance, and refractive index detectors. *Methods Mol. Biol. 328*, 97–112.
27. Zhou, J., and Xu, Z. (2003) Structural determinants of SecB recognition by SecA in bacterial protein translocation. *Nat. Struct. Biol. 10*, 942–947.
28. Lecker, S. H., Driessen, A. J., and Wickner, W. (1990) ProOmpA contains secondary and tertiary structure prior to translocation and is shielded from aggregation by association with SecB protein. *EMBO J. 9*, 2309–2314.
29. Tomkiewicz, D., Nouwen, N., and Driessen, A. J. (2008) Kinetics and energetics of the translocation of maltose binding protein folding mutants. *J. Mol. Biol. 377*, 83–90.
30. Panse, V. G., Swaminathan, C. P., Surolia, A., and Varadarajan, R. (2000) Thermodynamics of substrate binding to the chaperone SecB. *Biochemistry 39*, 2420–2427.
31. Ullers, R. S., Luirink, J., Harms, N., Schwager, F., Georgopoulos, C., and Genevaux, P. (2004) SecB is a bona fide generalized chaperone in *Escherichia coli*. *Proc. Natl. Acad. Sci. U.S.A. 101*, 7583–7588.
32. Krishnan, B., Kulothungan, S. R., Patra, A. K., Udgaonkar, J. B., and Varadarajan, R. (2009) SecB-mediated protein export need not occur via kinetic partitioning. *J. Mol. Biol. 385*, 1243–1256.